Catal Lett (2007) 119:108–119
DOI 10.1007/s10562-007-9206-6

Catalytic Conversion of NO and C_3H_6 in Exhaust Gases Over Silver Catalysts Under Stoichiometric or Excess Oxygen

Runduo Zhang · Houshang Alamdari · Serge Kaliaguine

Received: 24 May 2007 / Accepted: 3 July 2007 / Published online: 25 July 2007

Abstract The role of Ag in simultaneously catalyzing NO reduction and C_3H_6 oxidation was shown to be strongly dependent on the redox properties of its local environment. Under an atmosphere of 1,000 ppm NO, 3,000 ppm C_3H_6, and 1% O_2 and a GHSV of 30,000 h^{-1}, a perovskite $La_{0.88}Ag_{0.12}FeO_3$ prepared by reactive grinding is active giving a complete NO conversion and 92% C_3H_6 conversion at 500 °C. These values are much higher than the NO conversion of 55% and C_3H_6 conversion of 45% obtained over a 3 wt.% Ag/Al_2O_3 catalyst under the same conditions. Under an excess of oxygen (10% O_2) a good SCR performance with a plateau of N_2 yield above 97% over a wide temperature window of 350–500 °C along with C_3H_6 conversion of 90% at 500 °C was observed over Ag/Al_2O_3, while minor N_2 yields (~10% at 250–350 °C) and high C_3H_6 conversions (reaching ~100% at 450 °C) were obtained over $La_{0.88}Ag_{0.12}FeO_3$. Abundant molecular oxygen is desorbed from Ag substituted perovskite after 10% O_2 adsorption as verified by O_2- temperature programmed desorption (TPD). This reflects the strongly oxidative properties of $La_{0.88}Ag_{0.12}FeO_3$, which lead to a satisfactory NO reduction at 1% O_2 due to the ease of nitrate formation but to a significant C_3H_6 combustion above that value. The formation of nitrate species over the less oxidizing Ag/Al_2O_3 was accelerated under an excess of oxygen resulting in an excellent lean NO reduction behavior. The redox properties of silver catalysts could be adjusted via mixing perovskite with alumina for an optimal elimination of both NO and C_3H_6 over the whole range of oxygen concentration between 0 to 10%.

Keywords NO reduction · C_3H_6 oxidation · Silver · Perovskite · Alumina · Redox properties · TPD · TPR

1 Introduction

Nitrogen oxides (NO_x) and hydrocarbons (HCs) emitted from motor vehicles can contribute to the formation of harmful photochemical smog in the sunshine, which may lead to serious damage to human health and the eco-environment [1]. Their elimination is therefore important and becomes one of the most challenging topics for researchers engaged in environmental catalysis. The internal combustion engines of motor vehicles are commonly divided into gasoline engine and diesel engine [2]. The pollutant emissions of the gasoline engine usually present a reductant/oxidant ratio close to stoichiometric. In these conditions the catalytic reduction of NO by HCs and CO using three-way catalysts (TWCs), usually composed of noble metals (Pt, Pd, and Rh) supported on alumina, is a mature technology for the purification of exhaust gases from the gasoline engine [3, 4]. Over the past three decades, perovskites were considered as promising substitutes to expensive noble metals showing comparable catalytic activities but having the advantages of low cost, high resistance to water vapor poisoning and thermal sintering compared to noble metal catalysts [5, 6]. Perovskite-type oxides have excellent redox properties because of their abundant surface anion vacancies, which can adsorb or desorb oxygen readily, leading to a good catalytic

R. Zhang · S. Kaliaguine (✉)
Department of Chemical Engineering, Laval University, Ste Foy, QC, Canada G1K 7P4
e-mail: serge.kaliaguine@gch.ulaval.ca

H. Alamdari
Nanox Inc., 4975 rue Rideau, Local 100, Quebec, Canada G2E 5H5

performance in both NO reduction and C_3H_6 oxidation. In recent contributions from our group, such perovskites as La(Fe, Mn, Co)$_{1-x}Cu_xO_3$ were tested under a simulated atmosphere of the gasoline engine exhaust at stoichiometric oxygen content [7–10]. Facing a potential energy crisis, the use of both gasoline and diesel engines in lean burn conditions (over stoichiometric oxygen content), which achieves a more complete combustion of fuel became a popular tendency [2]. NO_x abatement under such oxidizing conditions is a great challenge for the conventional TWCs because it requires the limited reductant to selectively react with NO rather than O_2.

Supported silver catalysts were thought as effective materials for lean NO_x reduction and were investigated intensively [11–15]. The state of Ag, which depends greatly on the support nature, silver loading, and preparation method, is crucial for the selective catalytic reduction (SCR) performance. Ag^+ ions and Ag_2O nanoparticles strongly bonded to alumina were shown to be active sites for SCR of NO by HCs. Both are abundant in catalysts with an optimal Ag loading of approximately 2–3 wt.% at high dispersion [16]. High surface area γ-alumina was regarded as a better support than ZrO_2 and TiO_2–ZrO_2 [17, 18]. The smaller pore size with narrower distribution observed on alumina could also be important factors resulting in a better SCR activity [19]. The main drawback of using Ag/Al_2O_3 was found to be a significant formation of CO, a harmful by-product due to the partial oxidation of HCs leading to limited NO reduction under stoichiometric O_2 [20].

Incorporation of Ag into a perovskite lattice via substitution is another method (in addition to Ag impregnation on alumina support) to obtain highly isolated Ag^+ ions, associated with a local perovskite environment favorable to the complete transformation of HCs. These Ag substituted perovskites are thus expected to be suitable materials for simultaneous elimination of NO and C_3H_6 at stoichiometric oxygen content although, according to our earlier report [7], they may show poor deNO_x activity at excess oxygen due to severe C_3H_6 combustion.

In the present study, series of Ag-containing compounds including $La_{0.88}Ag_{0.12}FeO_3$, Ag/Al_2O_3, their parent $LaFeO_3$ and Al_2O_3, and the mixture of 10% $La_{0.88}Ag_{0.12}FeO_3$ + 90% Al_2O_3 (denoted as M(1P-9A) in this paper) were investigated to clarify the role of Ag and its local environment on the catalytic removal of NO and C_3H_6. The reference catalysts were characterized by X-ray diffraction (XRD), temperature programmed desorption (TPD) of O_2 and NO + O_2, temperature programmed reduction (TPR) by H_2, scanning electron microscopy (SEM) as well as activity tests towards NO reduction by C_3H_6 in the presence of 0–10% oxygen. An attempt to eliminate NO at high oxygen concentration using $La_{0.88}Ag_{0.12}FeO_3$ via an addition of reducing agent was also conducted.

2 Experimental

2.1 Preparation Method

$LaFeO_3$ and $La_{0.88}Ag_{0.12}FeO_3$ perovskites were prepared by reactive grinding of fully mix powders of La_2O_3 (Alfa, 99.99%), Fe_2O_3 (Baker & Adamson, 97.49%) and Ag_2O (Aldrich, 99.98%) via a high-energy-ball milling. This grinding process was conducted in two steps of 8 h for synthesis and 10 h for refining with a leachable additive of ZnO, as described in reference [21]. Alumina supported silver (Ag/Al_2O_3) with a loading of 3 wt.% was prepared by impregnating commercial boehmite (AlOOH) (Catapal 18N80) with an aqueous solution containing the desired amount of silver nitrate (99%, Aldrich) under 2 h stirring. Water was removed gradually through vacuum evaporation. The residue is dried at 110 °C for 4 h and calcined at 500 °C for 5 h. This procedure is also suitable for preparation of Al_2O_3 (without adding $AgNO_3$) or 3% $Ag/LaFeO_3$ (substituting $LaFeO_3$ for alumina support). The M(1P-9A) was prepared by mixing $La_{0.88}Ag_{0.12}FeO_3$ perovskite with Al_2O_3 under a weight ratio of 1:9 as a suspension in water. The final product was obtained after vacuum evaporation, 110 °C drying and 500 °C calcination.

2.2 Characterization of the Prepared Materials

BET surface areas of the materials calcined at 500 °C for 5 h were determined from the nitrogen adsorption/desorption isotherm at –196 °C using an automated gas sorption system (NOVA 2000, Quantachrome). The specific surface area was determined from the linear part of the BET curve (P/P_0 = 0.01–0.10).

The Ag content of samples was determined by atomic absorption spectroscopy (AAS) using a Perkin-Elmer 1100B spectrometer after the samples were dissolved in a mixture of 25 mL of 10% HCl and 2 mL of concentrated HF at 60 °C for 24 h.

XRD patterns of powders were recorded using a Siemens D 5,000 diffractometer and Cu Kα radiation (λ = 1.5406Å) with a 0.05° step scan from 20 to 80° in 2θ angle. The identification of the crystal phases was performed using the JCPDS data bank.

The morphology of the prepared samples after calcination at 500 °C for 5 h was studied by SEM, using a JEOL JSM 840A at 110 kV. Back scattered electrons (BSE) were captured to distinguish the region of $La_{0.88}Ag_{0.12}FeO_3$ from Al_2O_3 in their blending.

Transient studies were carried out with a multifunctional catalyst testing and characterization system (RXM-100, ASDI), equipped with a quadrupole mass spectrometer (MS) (UTI 100) and a thermal conductivity detector (TCD). Prior to H_2-TPR, the samples (50 mg) were pretreated under

10% O_2/He flow at 20 cm^3/min total flow rate for 1 h at 500 °C, cooled down to room temperature under the same atmosphere, purged with 20 cm^3/min of helium for 40 min to remove the physisorbed O_2, and then heated under a 20 cm^3/min total flow rate of 5% H_2/Ar stream with temperature rising up to 900 °C at a constant heating rate of 5 °C/min. H_2 consumption was monitored continuously using the TCD and a flow of 5% H_2/Ar at 20 cm^3/min as reference gas.

Prior to the TPD of O_2 and NO + O_2, the samples (50 mg) were treated under an atmosphere of 10% O_2, and 3,000 ppm NO + (1% or 10%) O_2, respectively, with a total flow rate of 20 cm^3/min at 500 °C for 1 h and then cooled down to room temperature under the same flow, subsequently, flushed with 20 cm^3/min He for 40 min to remove the physisorbed molecules. The temperature was then raised up to 800 °C for O_2-TPD and 500 °C for NO + O_2-TPD at a rate of 10 °C/min. O_2 and NO desorbed during TPD experiments were simultaneously detected and on-line recorded using MS with the mass numbers of 32 and 30, respectively.

2.3 Activity Measurements

The catalytic tests were performed in a fixed bed quartz reactor under an atmosphere of 1000 ppm NO, 3,000 ppm C_3H_6, and 0–10% O_2, balanced by He at a space velocity of 30,000 h^{-1}. The effluent gases (N_2O, NO_2, CO and C_3H_6) were analyzed using a FT-IR spectrometer (FTLA 2000 ABB Inc). N_2 and O_2 were monitored by gas chromatograph (GC) (HP 5890) equipped with TCD and separated by columns of molecular sieve 13X and Silicone OV-101. Nitrogen oxides (NO, NO_2) were also analyzed using a chemiluminescence $NO/NO_2/NO_x$ analyzer (Model 200AH, API). Organo nitrogen compounds (ONCs), mentioned in the literature as intermediates of NO reduction by HCs [22–24], can be detected by comparing the different NO_2 values from the NO_x analyzer with that from the IR spectrometer as demonstrated in our earlier report [7].

3 Results

3.1 Catalysts Characterization

3.1.1 Physicochemical Properties

The crystal phase was established by XRD (Fig. 1), revealing a main orthorhombic $LaFeO_3$ perovskite-type structure (JCPDS 74-2203) for $LaFeO_3$ and $La_{0.88}Ag_{0.12}FeO_3$. No diffraction line corresponding to Ag_2O (JCPDS 41-1104) and Ag (JCPDS 04-0783) was observed for $La_{0.88}Ag_{0.12}FeO_3$, suggesting that Ag metal was fully incorporated into the perovskite structure of $LaFeO_3$ or the formed particles were too tiny to be detected by XRD. However, diffraction peaks of metallic Ag were observed in the XRD pattern of $Ag/LaFeO_3$, indicating silver is mainly dispersed as metallic Ag after its impregnation over $LaFeO_3$ perovskite. Both Al_2O_3 and Ag/Al_2O_3 prepared from boehmite showed γ-Al_2O_3 structure (JCPDS 29-0063) in their XRD patterns. No XRD peak related to Ag_2O and Ag was observed reflecting a high dispersion of silver over support likely via a strong interaction between silver and alumina.

The BET surface areas of the prepared materials are reported in Table 1, showing a specific surface area of 31 m^2/g for the $LaFeO_3$ after calcination at 500 °C. About 12% Ag substitution led to an increase in surface area yielding a value of 37 m^2/g for $La_{0.88}Ag_{0.12}FeO_3$. About 3% Ag impregnation over $LaFeO_3$ resulted in a decrease in surface area giving a value of 8 m^2/g for $Ag/LaFeO_3$. Ag impregnation and 10% $La_{0.88}Ag_{0.12}FeO_3$ blend hardly affected the surface area of Al_2O_3 (143 m^2/g for Al_2O_3, 140 m^2/g for Ag/Al_2O_3, and 140 m^2/g for M(1P-9A)). It is noticeable that just one third of the initial surface area of $La_{0.88}Ag_{0.12}FeO_3$ is left after C_3H_6 + NO + O_2 reaction at 700 °C. With the mixing of $La_{0.88}Ag_{0.12}FeO_3$ with alumina, the prepared mixture could maintain ~80% of its original surface area after undergoing a 700 °C reaction.

Ag impregnation decreases the surface area of $LaFeO_3$ from 31 to 8 m^2/g, which is a normal phenomenon for the impregnation process due to the coverage of surface by low-surface clusters of active component. Contrastively, Ag substitution does improve the surface area of $LaFeO_3$, suggesting that Ag has mainly been incorporated into the perovskite lattice in accordance with XRD results. Only a slight decrease in surface area was observed after Ag impregnation over Al_2O_3. This was attributed to the high surface area of the alumina support, which leads to a good dispersion of Ag component. On the contrary, the appearance of Ag^0 peak in the XRD pattern of $Ag/LaFeO_3$ was related to the relatively low surface area of $LaFeO_3$. Ag contents of silver-containing catalysts determined by AAS and listed in Table 1 are close to the nominal values.

SEM pictures indicated that Al_2O_3 particles have almost regular spherical shape with a size of 30–200 nm (not shown). This morphology hardly changed after Ag impregnation (Fig. 2a). Ag particles weren't observed from the XRD pattern of Ag/Al_2O_3, implying that impregnated Ag was well dispersed over the support (as Ag^+ or fine Ag_2O) and therefore invisible due to the SEM limited resolution. A sponge-like phase with irregular clusters, thought to be composed of individual nanoscale primary particles according to our previous description [25], was observed for $La_{0.88}Ag_{0.12}FeO_3$ in Fig. 2b. Some $La_{0.88}Ag_{0.12}FeO_3$ (white region) embedded with Al_2O_3

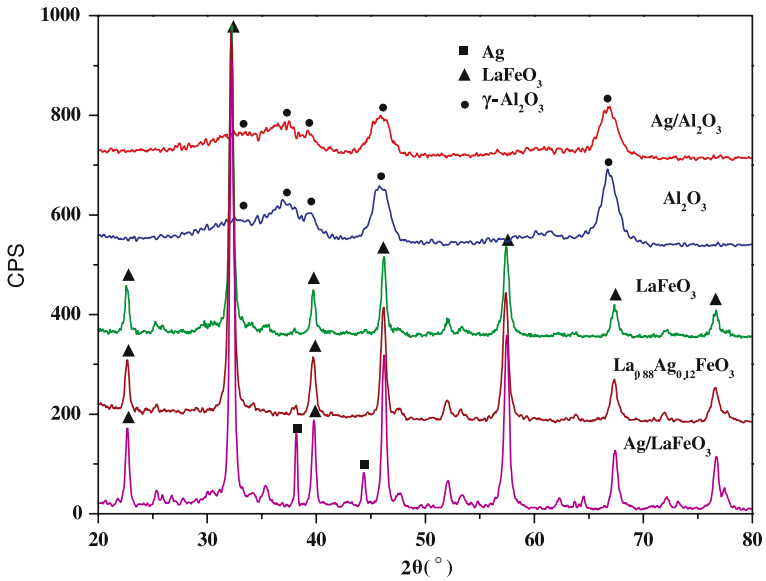

Fig. 1 XRD patterns of prepared solid solutions

Table 1 Physicochemical properties of prepared catalysts after calcination at 500 °C for 5 h

Sample	Specific surface area (m^2/g)	Ag content (wt.%)	Amount of oxygen desorbed during O_2-TPD		
			α-O_2 (μmol/g)	β-O_2 (μmol/g)	Total (μmol/g)
$LaFeO_3$	31	–	41 (<700 °C)	75 (700–800 °C)	116
$La_{0.88}Ag_{0.12}FeO_3$	37	5.1	117 (564 °C)	219 (799 °C)	336
Al_2O_3	143	–	–	4 (736 °C)	4
Ag/Al_2O_3	140	2.9	–	14 (693 °C)	14
Mixture (1P-9A)	140	0.5	2 (352 °C)	9 (608 °C)	11
$Ag/LaFeO_3$	8	3.2			

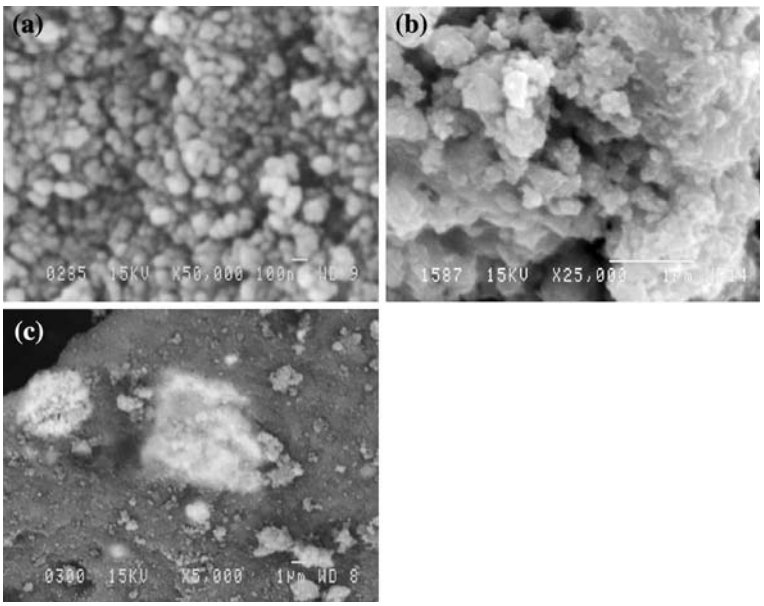

Fig. 2 TEM of (**a**) Ag/Al_2O_3, ×50,000, (**b**) $La_{0.88}Ag_{0.12}FeO_3$, ×25,000, (**c**) Mixture of 10% $La_{0.88}Ag_{0.12}FeO_3$ + 90% Al_2O_3, ×5,000 (BSE)

(gray region) may be distinguished from Fig. 2c exhibiting a special structure with different catalytic phases for this bi-component M(1P-9A).

3.1.2 Temperature Programmed Analyses

The various O_2 species formed over the prepared catalysts were investigated by O_2-TPD experiments, as illustrated in Fig. 3. The O_2 desorbed (41 μmol/g) from $LaFeO_3$ at <700 °C is designated as α-O_2 and ascribed to oxygen species bound to the surface anion vacancies of perovskite, whereas the O_2 desorbed (75 μmol/g) at >700 °C is referred to as β-O_2 attributed to oxygen species liberated from the lattice as discussed in our previous studies [26]. Compared to $LaFeO_3$, a higher α-O_2 desorption (117 μmol/g) together with an enhanced β-O_2 desorption (219 μmol/g) was observed in the O_2-TPD profile for $La_{0.88}Ag_{0.12}FeO_3$ perovskite. This significant enhancement of α-O_2 amount is likely related to the newly generated oxygen vacancies upon Ag substitution due to a positive charge compensation [27], while the improvement in β-O_2 desorption was ascribed to the higher mobility of lattice oxygens associated with Ag ions compared to those associated with Fe ions.

Oxygen desorption from alumina-based catalysts were in much lower amounts than those occurring over Fe-based perovskites (Fig. 3 and Table 1). This result reflects a poorer oxidizing capacity of alumina with respect to perovskite, possibly resulting in different catalytic performances in the corresponding redox reactions. A single O_2 peak (4 μmol/g) at 736 °C was observed in the O_2-TPD profile of Al_2O_3. This oxygen adsorption was facilitated by Ag impregnation representing as a peak (14 μmol/g) at 693 °C. The blend of Al_2O_3 with $La_{0.88}Ag_{0.12}FeO_3$ led to the occurring of α-O_2 desorption, O_2 peak (2 μmol/g) at 352 °C followed by another (9 μmol/g) at 608 °C (line (e) in Fig. 3).

The reducibility of the prepared solids was investigated by H_2-TPR experiments. The results are shown in Fig. 4. A multi-step reduction was observed for $LaFeO_3$, showing an intense peak at 560 °C and a shoulder at 376 °C, and an incomplete one at 877 °C which were respectively ascribed the reduction of $Fe^{3+} \rightarrow Fe^{2+}$, $Fe^{4+} \rightarrow Fe^{3+}$ and partial $Fe^{2+} \rightarrow$ metallic iron according to our earlier ascription of TPR peaks for the same compound [7].

After partial substitution of La ions in lanthanum ferrite by Ag ions, one minor peak at 127 °C, followed by a sharp peak at 413 °C overlapping with one at 490 °C, and two superimposed peaks at 780 and 900 °C were observed. Based on the assignment of TPR peaks for $LaFeO_3$, the sharp peak at 413 °C observed in the TPR profile of $La_{0.88}Ag_{0.12}FeO_3$ was ascribed to the reduction of Ag^{2+} to Ag^0 in perovskite lattice. The $Fe^{3+} \rightarrow Fe^{2+}$ reduction peak was shifted to lower temperature (490 °C) in Ag-substituted sample, suggesting that the lattice Ag^0 produced at this temperature resulted in an easier reduction of Fe^{3+}. The H_2 consumption above 700 °C was again attributed to $Fe^{2+} \rightarrow Fe^0$ reduction. Finally, the minor TPR peak at 127 °C was likely due to the reduction of some large-size Ag_2O particles over perovskite according to literature [28]. It is therefore thought that Ag was mainly incorporated into perovskite lattice with some minor silver oxides segregated over the surface.

Unlike lanthanum ferrites, Al_2O_3 seems to be irreducible over the tested temperature range (<900 °C) (line (c) in Fig. 4) corresponding to the low mobility of its lattice oxygen. This can be slightly improved by $La_{0.88}Ag_{0.12}FeO_3$ blend (line (e) in Fig. 4). Richter et al. [28] pointed out that

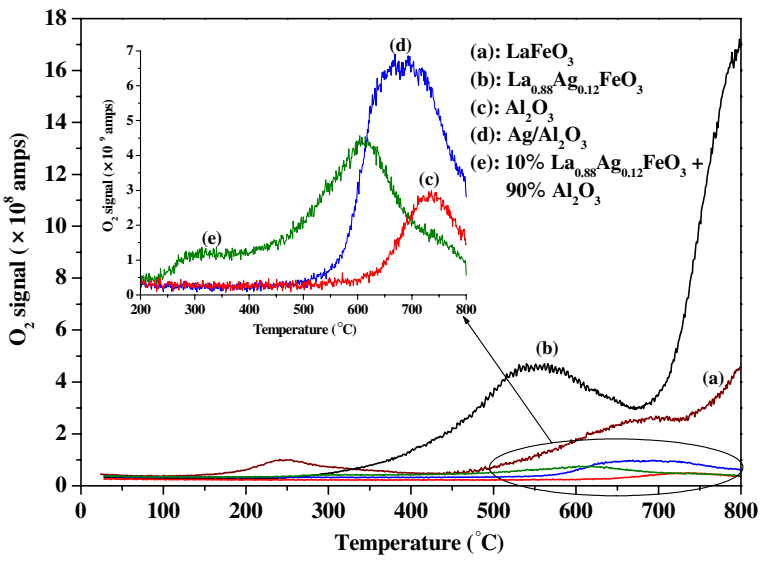

Fig. 3 TPD of O_2 profiles over prepared catalysts

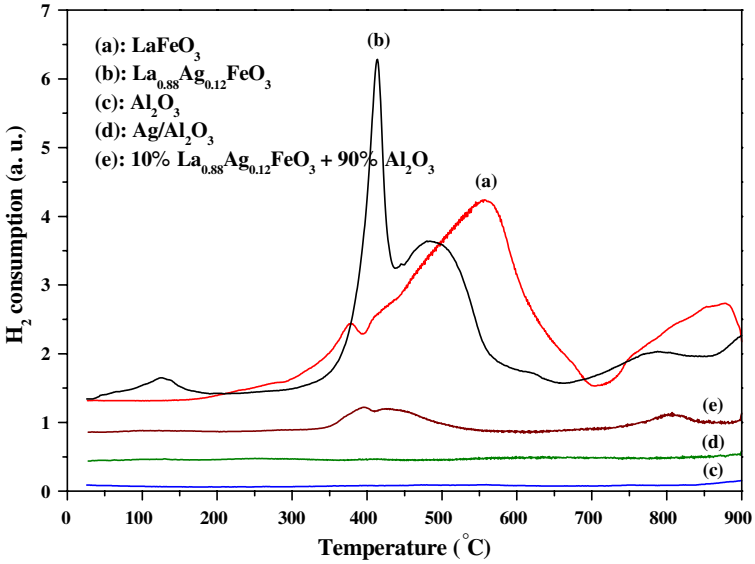

Fig. 4 H_2-TPR profiles of prepared catalysts

Ag_2O clusters supported on alumina are increasingly stabilized against reduction with the diminution of their particle sizes. In this study, no obvious TPR peak related to silver was observed at $T < 900$ °C over Ag loaded alumina (line (d) in Fig. 4). This result indicates that the present preparation method produces highly dispersed silver, possibly as Ag^+ or nanoscale Ag_2O via a strong interaction with the alumina support as documented in the literature [13, 14, 29].

Figure 5 shows the desorption signal for NO (m/e = 30) during the NO-TPD test after the co-adsorption of NO/O_2. Three peaks at 105, 250, and 377 °C were observed in the NO desorption trace of $La_{0.88}Ag_{0.12}FeO_3$ after an adsorption of 3,000 ppm NO and 1% O_2 and were respectively ascribed to physisorbed NO, nitrosyl and nitrate species in the order of their thermal stability according to the literature [13]. Only two significant peaks at 180 and 354 °C were observed in the NO desorption trace of Ag/Al_2O_3 after 3,000 ppm NO and 1% O_2 adsorption and were accordingly assigned to the desorptions of nitrosyl and nitrate species according to their desorption temperatures. Nitrate species, which are regarded as important intermediates for SCR of NO by propene [16, 30], are more easily formed over $La_{0.88}Ag_{0.12}FeO_3$ compared to Ag/Al_2O_3 under an atmosphere of 3,000 ppm NO and 1% O_2 as shown in Fig. 5. This result is likely related to the excellent oxidizing properties of perovskite exhibiting as the abundant α-O_2 desorption in its O_2-TPD pattern (Fig. 3). These oxygen species bound to surface vacancies (α-O_2) are believed to be able to oxidize adsorbed NO into NO_3^- species [7]. Interestingly, the high-temperature NO peak (at 383 °C) assigned to NO_3^- species formed over Ag/Al_2O_3

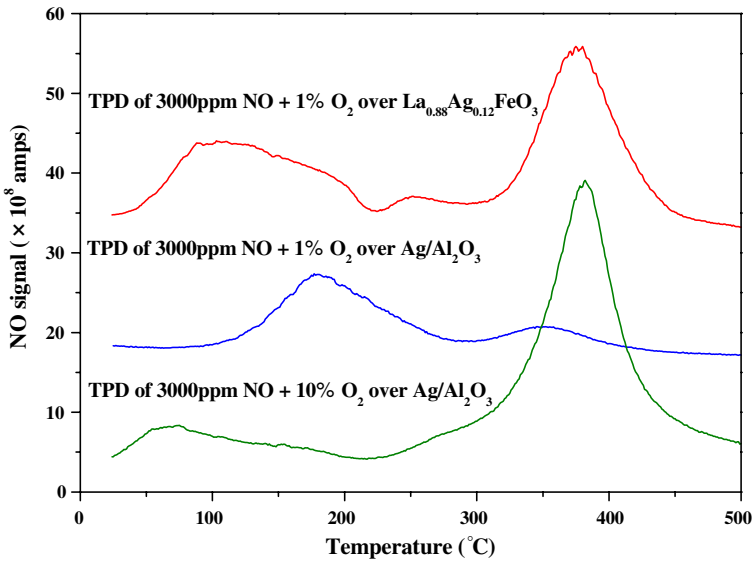

Fig. 5 TPD of NO + O_2 profiles over $La_{0.88}Ag_{0.12}FeO_3$ and Ag/Al_2O_3

was significantly enhanced during NO + O_2-TPD with adsorption in the presence of 10% O_2. This suggests that the formation of nitrate species over poorly oxidizing alumina could be promoted by means of introducing more molecular oxygen into the gas phase. Two minor peaks at 67 and 155 °C in the TPD profile of 3,000 ppm NO + 10% O_2 for Ag/Al_2O_3 were subsequently assigned to physisorbed NO and nitrosyl species.

3.2 Activity Tests

3.2.1 Reduction Under Conditions Close to Stoichiometry (1% O_2)

A comparative study of NO catalytic reduction by propene in the presence of 1% O_2 was carried out over $LaFeO_3$, $La_{0.88}Ag_{0.12}FeO_3$, Al_2O_3, Ag/Al_2O_3 and M(1P-9A) (Fig. 6a–c) in order to clarify the role of Ag location in distinct environments (perovskite lattice and alumina surface) on the catalytic performance. The temperature dependence of NO conversion is shown in Fig. 6a. NO conversion for $LaFeO_3$ started at 200 °C and increased progressively with temperature, reaching 52% at 450 °C and 92% at 500 °C. A moderate enhancement was observed over lanthanum ferrite after Ag partial substitution, resulting in a NO conversion of 68% at 450 °C and 100% at 500 °C. A relatively lower NO conversion was obtained over Al_2O_3 initiated at about 400 °C and only becoming significant at $T > 600$ °C. About 3% Ag loading over this Al_2O_3 support obviously improved NO conversions at low temperatures (300–600 °C) resulting in a maximum of 55% at 500 °C but scarcely affecting these conversions above 600 °C. Nevertheless, NO conversions obtained over Ag-promoted alumina were still lower than those values for Fe-based perovskites especially at the temperature range of 450–650 °C. With 10% $La_{0.88}Ag_{0.12}FeO_3$ blend into alumina, the obtained mixture showed an activity curve of NO conversion similar to that of $La_{0.88}Ag_{0.12}FeO_3$ alone.

N_2 formation is significant at >400 °C for $LaFeO_3$ and >550 °C for Al_2O_3 (not shown). Ag addition facilitated the N_2 production resulting in three similar N_2 yield curves for Ag/Al_2O_3, $La_{0.88}Ag_{0.12}FeO_3$ and M(1P-9A). Less ONCs were generated over alumina compared to $LaFeO_3$ (not shown). Supported Ag slightly facilitated the ONCs formation over Al_2O_3, while Ag substitution led to a shift of ONCs yield achieved over $LaFeO_3$ to low temperature. ONCs yields obtained over M(1P-9A) were obviously

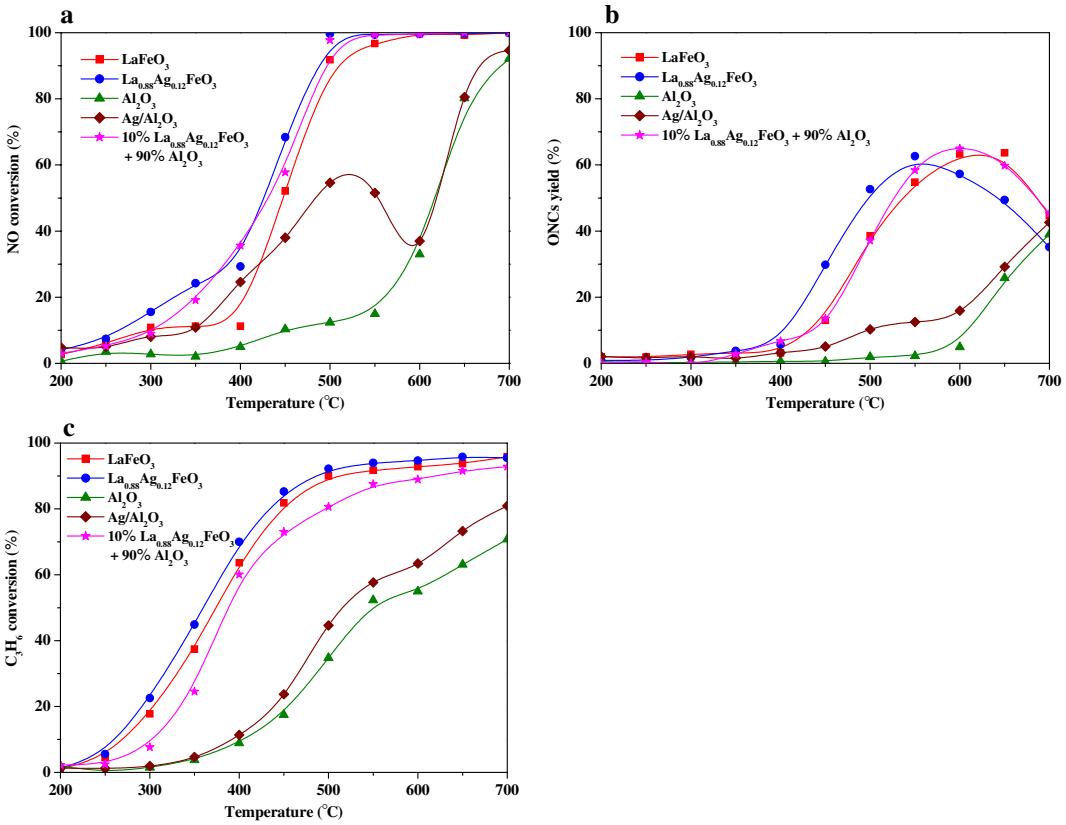

Fig. 6 (**a**) NO conversion, (**b**) ONCs yield, (**c**) C_3H_6 conversion in C_3H_6 + NO + O_2 reactions over $LaFeO_3$, $La_{0.88}Ag_{0.12}FeO_3$, Al_2O_3, Ag/Al_2O_3, and mixture of 10% $La_{0.88}Ag_{0.12}FeO_3$ + 90% Al_2O_3. Conditions: GHSV = 30,000 h^{-1}, 3,000 ppm C_3H_6, 1,000 ppm NO, 1% O_2

enhanced (compared to that obtained over Al_2O_3) and the maxima of their ONCs yield were slightly shifted to higher temperature with respect to $La_{0.88}Ag_{0.12}FeO_3$ (Fig. 6b).

A progressive increase in C_3H_6 conversion at increasing temperature and up to 71% at 700 °C was found in the case of Al_2O_3 (Fig. 6c). C_3H_6 conversions were further improved by means of Ag impregnation resulting in a value of 81% at 700 °C for Ag/Al_2O_3. The blend of $La_{0.88}Ag_{0.12}FeO_3$ [M(1P-9A)] significantly increased the C_3H_6 conversion compared to Al_2O_3 (Fig. 6c). Compared to alumina-based catalysts, much higher C_3H_6 conversions were obtained with values reaching 90% and 92% at 500 °C for $LaFeO_3$ and $La_{0.88}Ag_{0.12}FeO_3$, respectively. On the contrary, CO due to partial oxidation of C_3H_6 was more easily formed at 1% O_2 over alumina-supported samples with respect to Fe-based perovskites (not shown). A depletion in CO yield occurred after the introducing $La_{0.88}Ag_{0.12}FeO_3$ into alumina substrate [M(1P-9A)] except for a minor CO yield appearing at around 400 °C.

3.2.2 *Reduction Under Lean Burn Conditions (10% O_2)*

The temperature dependence of NO and C_3H_6 conversions as well as N_2, ONCs, and NO_2 yields in a feed flow of 1,000 ppm NO + 3,000 ppm C_3H_6 + 10% O_2 over $LaFeO_3$, $La_{0.88}Ag_{0.12}FeO_3$, Al_2O_3, Ag/Al_2O_3, and M(1P-9A) are depicted in Fig. 7a–c. NO conversion was marginal over $LaFeO_3$ at <400 °C and 10% O_2 (Fig. 7a). Ag-substituted perovskite showed NO conversions of ~10% at 250–350 °C and ~18% 650–700 °C. NO conversion of $La_{0.88}Ag_{0.12}FeO_3$ was improved by mixing with Al_2O_3 resulting in a value of ~30% at >400 °C which suggests one means of using perovskite into the NO abatement in excess oxygen. In the case of alumina, significant NO conversion started at 450 °C, passed through a maximum of 85% at 500 °C before its diminution. A high N_2 yield was achieved over Ag/Al_2O_3 showing a plateau of >97% over a wide temperature window from 350 to 500 °C. The order for N_2 yields (not shown) obtained over these catalysts was similar to that for the above mentioned NO conversions. ONCs yields are minor (<2%) in the case of lanthanum ferrites (Fig. 7b). Over Ag/Al_2O_3 ONCs appeared at $T < 500$ °C with a maximum of 11% at 300 °C, while over Al_2O_3 ONCs yield was only significant at $T > 500$ °C showing a maximum of 34% at 600 °C. Unlike the results obtained in 1% O_2 which exhibited a positive effect on ONCs generation by addition perovskite (Fig. 6 b), the addition of $La_{0.88}Ag_{0.12}FeO_3$ into Al_2O_3 inhibited

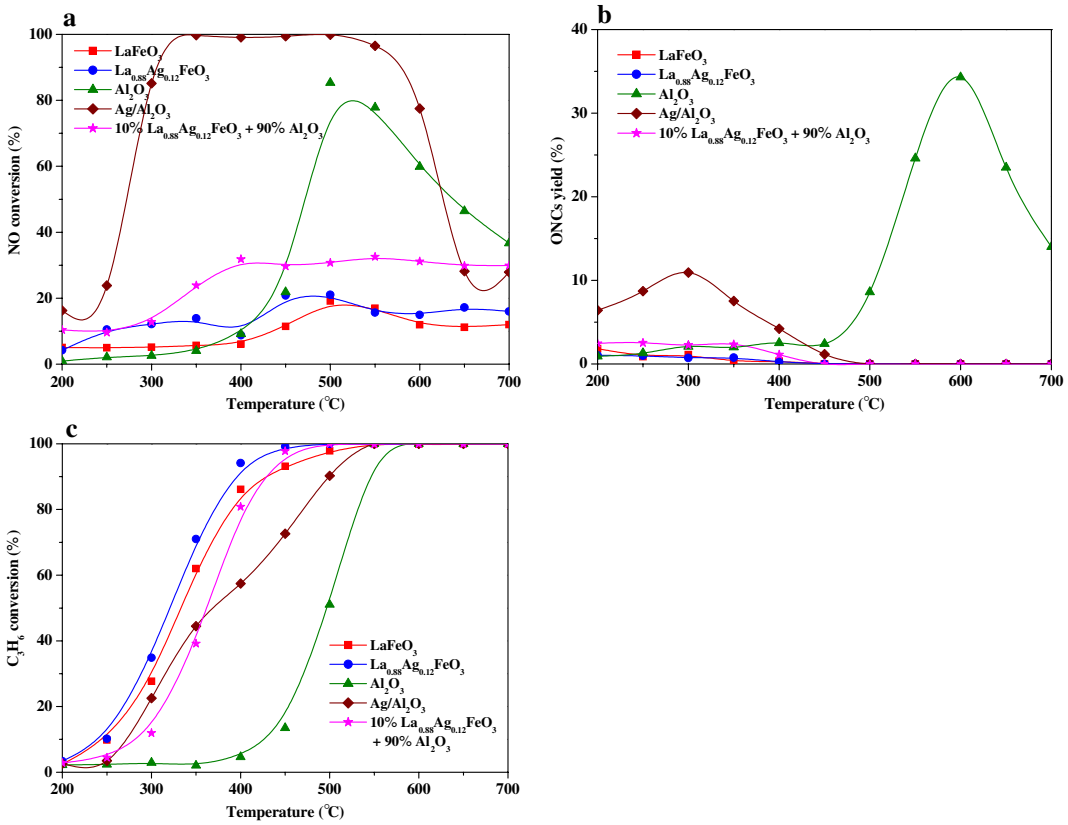

Fig. 7 (**a**) NO conversion, (**b**) ONCs yield, (**c**) C_3H_6 conversion in C_3H_6 + NO + O_2 reactions over $LaFeO_3$, $La_{0.88}Ag_{0.12}FeO_3$, Al_2O_3, Ag/Al_2O_3, and mixture of 10% $La_{0.88}Ag_{0.12}FeO_3$ + 90% Al_2O_3. Conditions: GHSV = 30,000 h^{-1}, 3,000 ppm C_3H_6, 1,000 ppm NO, 10% O_2

the appearance of ONCs under a 10% O_2 containing atmosphere (Fig. 7b). NO_2 is another kind of N-containing compound detected during C_3H_6-SCR of NO in excess oxygen (not shown). It was seen that the NO_2 formation was easier at 10% O_2 with maxima of 16% and 18% at 500 °C for $LaFeO_3$ and $La_{0.88}Ag_{0.12}FeO_3$. NO_2 generation over Al_2O_3 and Ag/Al_2O_3 occurred at relatively higher temperature (>500 °C). This coincides with the fact that the nitrate species formed over $La_{0.88}Ag_{0.12}FeO_3$ perovskite are more abundant than on Ag/Al_2O_3 as established by NO + O_2-TPD (Fig. 5). An enhancement in NO_2 yield was found after adding perovskite into alumina (not shown). C_3H_6 conversion over the tested samples in Fig. 7c followed the order of $La_{0.88}Ag_{0.12}FeO_3$ > $LaFeO_3$ > M(1P-9A) > Ag/Al_2O_3 > Al_2O_3 in agreement with their oxidizing abilities as evidenced by O_2-TPD (Fig. 3).

3.2.3 *Reduction Under Conditions Ranging from Rich Burn to Lean Burn*

The effect of oxygen concentration on NO and C_3H_6 conversions, N_2, ONCs and NO_2 yields at 500 °C over $La_{0.88}Ag_{0.12}FeO_3$ was compared at two different concentrations of C_3H_6 under an atmosphere of 1,000 ppm NO, 0–10% O_2, and 3,000 ppm or 6,000 ppm C_3H_6 (Fig. 8a and b). Using 3,000 ppm C_3H_6 (Fig. 8a), an almost complete NO conversion towards N_2 and ONCs products was obtained at O_2 feed concentration ≤1%. ONCs yield was slightly improved by 1% O_2, however, it was totally suppressed at higher oxygen concentrations. As oxygen concentration is higher than 1%, the NO conversion rapidly diminishes and NO_2 is the main N-containing compound in effluent at O_2 content >4%. C_3H_6 conversion was significantly enhanced by 1% O_2 addition into the feed compared to that obtained in the absence of oxygen. A moderate decline in C_3H_6 conversion from 92% to 71% as O_2 feed concentration increases from 1% up to 2% simultaneously with a diminution of ONCs yield, suggesting the transformation of C_3H_6 into ONCs makes a main contribution to C_3H_6 conversion as O_2 concentration is less than 2%, while C_3H_6 conversion is accelerated by gaseous O_2 via a complete oxidation at higher O_2 partial pressure.

The catalytic behavior in NO + C_3H_6 + O_2 reaction after switching C_3H_6 concentration from 3,000 ppm to 6,000 ppm is illustrated in Fig. 8b. In the presence of 6,000 ppm C_3H_6, both NO conversion and N_2 yield are improved achieving a NO conversion of 99% and N_2 yield of 71% at 2% O_2. A comparison of NO conversions in

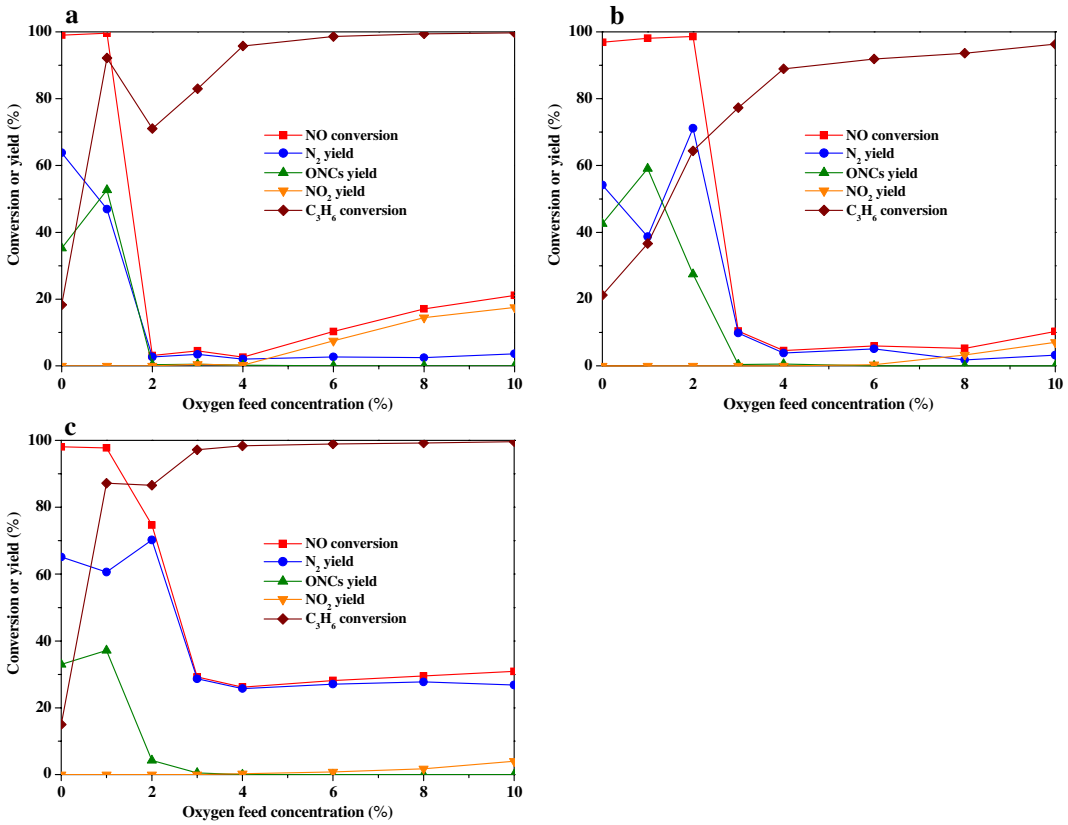

Fig. 8 Effect of O_2 feed concentration on catalytic behavior in C_3H_6 + NO + O_2 reactions. Conditions: GHSV = 30,000 h^{-1}, T = 500 °C, 1,000 ppm NO (**a**) 3,000 ppm C_3H_6 over $La_{0.88}Ag_{0.12}FeO_3$, (**b**) 6,000 ppm C_3H_6 over $La_{0.88}Ag_{0.12}FeO_3$, (**c**) 3,000 ppm C_3H_6 over mixture of 10% $La_{0.88}Ag_{0.12}FeO_3$ + 90% Al_2O_3

Fig. 8a and b indicates that a good deNO_x effectiveness of perovskite even at relatively higher oxygen concentrations can be maintained by increasing the reducing agent. By contrast, the C_3H_6 conversion and NO_2 yield were slightly inhibited after the C_3H_6 concentration is increased from 3,000 to 6,000 ppm.

The catalytic performances of NO and C_3H_6 conversions, N_2, ONCs and NO_2 yields at 500 °C as functions of O_2 feed concentration over the mixture of 10% $La_{0.88}Ag_{0.12}FeO_3$ and 90% alumina are shown in Fig. 8c. As seen from Fig. 8c, M(1P-9A) maintained a NO conversion of 75% at 2% O_2 and ~30% at >3% O_2. N_2 yields of 60–70% at 0–2% O_2 associated with a maximum ONCs yield of 37% at 1% O_2 were observed. At >3% O_2, the ONCs formation was totally inhibited resulting in similar values between NO conversion and N_2 yield. A satisfactory C_3H_6 conversion was also achieved over the tested mixture which reached 87% at 1% O_2 and further increased at higher O_2 feed concentrations (Fig. 8c).

4 Discussion

4.1 Relation Between Redox Properties of $LaFeO_3$ and Al_2O_3 with their Catalytic Performance

A mechanism for NO catalytic reduction by propene in the presence of oxygen was previously proposed for Fe, Mn and Co-based perovskites involving ONCs, likely generated from the interaction between nitrate species and adsorbed C_3H_6. Subsequently, an isocyanate intermediate forms from ONCs and reacts with NO and/or O_2 to get the final products [7–9]. Similar mechanism for C_3H_6-SCR of NO in excess oxygen over alumina-based catalysts was documented in the literature with the formation of nitrate species (or NO_2) as the first important step and R-NCO as a key intermediate [30].

The distinct redox properties of $LaFeO_3$ perovskite and Al_2O_3 were illustrated by O_2-TPD (Fig. 3). Those α-oxygens formed over perovskite are believed to be responsible for good oxidative properties and facilitate both the nitrate formation and the propene oxidation [7, 26], while lattice oxygen becomes removable and reactive merely at high temperature (>700 °C). By contrast, the O_2 desorption from alumina occurs merely at relatively high temperature (736 °C) underlining its poor oxidative ability.

A satisfactory performance was achieved over $LaFeO_3$ with a NO conversion of 52% at 450 °C and 92% at 500 °C simultaneously with a C_3H_6 conversion of 85% at 450 °C and 92% at 500 °C under an oxygen atmosphere close to stoichiometry (1% O_2). A rather poor NO conversion, which only became noticeable at $T > 600$ °C, was however found in the case of Al_2O_3 under the above experimental conditions. According to the above reported mechanism, the NO → nitrate (or NO_2) oxidation is an important step for NO catalytic reduction by propene in the presence of oxygen [7, 16, 30]. Nitrate species can be readily formed under an atmosphere containing 3,000 ppm NO and 1% O_2 over Fe-based perovskites because of its good oxidizing ability, while nitrate species formed over Al_2O_3-related samples undergoing the same pretreatment was scarce as verified by NO + O_2-TPD (Fig. 5). These nitrate species over $LaFeO_3$ are important for ONCs generation (Fig. 6b) as described by our previous mechanism according to which ONCs are generated via an interaction between nitrate species and adsorbed C_3H_6 [7]. In general, the distinct oxidative properties between $LaFeO_3$ and Al_2O_3 resulted in different surface concentrations of nitrate species formed, resulting in different catalytic behaviors in NO reduction by propene under 1% O_2. A relatively lower C_3H_6 conversion of 71% along with apparent CO yield of 15% at 700 °C was obtained over Al_2O_3 compared to that obtained over $LaFeO_3$. The generation of CO is an indication of partial oxidation of C_3H_6 under 1% O_2. Those results were again in agreement with the less oxidizing properties of alumina compared to $LaFeO_3$.

It is seen from Fig. 7a that NO conversion over $LaFeO_3$ perovskite became marginal under an excess of oxygen (10% O_2). The depletion of reducing agent necessary for NO reduction via a complete oxidation by oxidative $LaFeO_3$ perovskite is thought to be the main reason for the suppression of NO conversion as discussed in our earlier report [7]. On the contrary, NO conversion over Al_2O_3 was obviously improved by a high oxygen concentration yielding a maximum of 85% at 500 °C. It was shown that the density of nitrate species over alumina-based samples could be significantly increased upon raising the oxygen concentration in the gas phase from 1% to 10% during NO + O_2-TPD tests (Fig. 5). The shift to low temperature of curves for N_2 and ONCs yields over Al_2O_3 obtained at 10% O_2 compared to those obtained at 1% O_2 was therefore attributed to the ease of nitrate formation at high oxygen concentration. An easier NO_2 formation together with a much higher C_3H_6 conversion (Fig. 7c) was observed over $LaFeO_3$ with respect to Al_2O_3. These behaviors in the oxidation of NO and C_3H_6 coincide with the oxidizing properties of these materials.

4.2 Role of Ag Located in Distinct Redox Environments

An enhanced α-O_2 desorption over lanthanum ferrite after Ag substitution was observed in the O_2-TPD pattern of Fig. 3. This was likely related to the generation of more anion vacancies caused by a positive charge compensation. Moreover, the mobility of lattice oxygen was also en-

hanced by this Ag incorporation into $LaFeO_3$ (Figs. 3 and 4). The anion vacancies are thought to be the active sites (adsorption sites for O_2 and NO) of perovskite during NO catalytic reduction [7, 31, 32]. Additionally, abundant molecular oxygen can accelerate nitrate formation which is crucial for C_3H_6 + NO + O_2 reaction and C_3H_6 oxidation [9]. This led to the promotion of NO and C_3H_6 conversions in the presence of 1% O_2 for $LaFeO_3$ via Ag substitution (Fig. 6a and c). Such a promotion in C_3H_6 conversion was also observed in the case of 10% O_2 (Fig. 7c). However, NO conversion obtained over $La_{0.88}Ag_{0.12}FeO_3$ under an excess of oxygen was again inhibited due to C_3H_6 depletion by combustion (Fig. 7a).

Ag promoted alumina shows a higher O_2 desorption occurring at relatively lower temperature in its O_2-TPD patterns (Fig. 3) with respect to Al_2O_3. This reflects the fact that oxygens associated with Ag ions have a higher mobility compared to those bound to Al ions, likely leading to an enhanced oxidizing ability of alumina via Ag impregnation consistent with the C_3H_6 conversions obtained over Al_2O_3 and Ag/Al_2O_3 (see Figs. 6c and 7c). Indeed, Ag dispersed over Al_2O_3 support effectively increases the low-temperature NO conversion under 1% O_2 yielding a maximum of 55% at 500 °C and affects less the conversion above 600 °C (Fig. 6a). In the presence of 10% O_2, high NO conversions with values >97% at 350–500 °C were also obtained over Ag/Al_2O_3. A bifunctional mechanism was proposed by Bethke and Kung with metal ions as sites for nitrate or adsorbed NO_2 formation and alumina providing sites for dinitrogen formation [14]. Thus, the promotion of catalytic performance (especially at low temperature) by Ag impregnation was realized via facilitating the formation of nitrate (or NO_2) species. Although several forms of silver can catalyze the NO reduction, Ag^+ or fine Ag_2O phase achieved through a high dispersion of active component is crucial for the selective reduction of NO to N_2. Metallic Ag present in larger particles promotes combustion of the reductant [13, 14, 28]. The role of high-surface alumina (143 m^2/g) is to maintain the Ag^+ or fine Ag_2O status via a strong interaction between silver and support. This opinion was also supported by the similarities of XRD and TPR patterns of Al_2O_3 and Ag/Al_2O_3 (Figs. 1 and 4).

4.3 Transformation of NO at Oxygen Concentrations Higher than Stoichiometric

$La_{0.88}Ag_{0.12}FeO_3$ has excellent oxidizing properties, showing good $deNO_x$ performance at approximately stoichiometric oxygen content. Nevertheless under excess oxygen, its NO reduction was totally inhibited due to a serious C_3H_6 combustion. Lean burn gasoline and diesel engine require catalytic materials able to achieve NO removal at high oxygen concentration, which seems to be a challenge for the practical application of perovskites in the purification of auto exhaust gases.

Since the detrimental effect of oxygen at its concentration higher than stoichiometric for perovskite-type catalysts is to consume the limited reducing agent leading to a deactivation in NO abatement, additional reducing agent can be fed to the catalyst to satisfy the requirement for NO reduction. In the presence of 3,000 ppm C_3H_6, an approximately complete NO conversion over $La_{0.88}Ag_{0.12}FeO_3$ was obtained at oxygen concentrations not exceeding 1% (Fig. 8a). At higher oxygen concentrations, NO conversion decreased drastically. With the increase of C_3H_6 feed concentration up to 6,000 ppm (Fig. 8b), $La_{0.88}Ag_{0.12}FeO_3$ can work well even at 2% O_2 showing a nearly complete NO conversion and an obviously enhanced N_2 yield (71%). The above results confirm our assumption that the catalytic behavior in NO reduction at O_2 concentrations higher than stoichiometric (e.g. exhaust gas from "lean burn" gasoline engine) over perovskite can be improved through additional injection of reducing agent.

4.4 Synergistic Effect of Perovskite and Alumina

Propene is oxidized not only to CO_2 but also to CO simultaneously with formation of nitrogen at approximately stoichiometric O_2 over alumina. CO formation is avoided over $La_{0.88}Ag_{0.12}FeO_3$ together with an improvement in NO reduction at 1% O_2. $DeNO_x$ activity of $La_{0.88}Ag_{0.12}FeO_3$ was however poor at 10% O_2 due to C_3H_6 combustion. The blend of $La_{0.88}Ag_{0.12}FeO_3$ and Al_2O_3 seems to be a good method to adjust the redox properties of catalysts to optimally eliminate both NO and C_3H_6 under the whole range of practical oxygen contents. The bi-component catalyst M(1P-9A) was prepared and expected to take $La_{0.88}Ag_{0.12}FeO_3$ as centers for nitrate formation and Al_2O_3 as sites for dinitrogen formation.

In the presence of 1% O_2, NO conversion over Al_2O_3 was obviously improved via only 10% $La_{0.88}Ag_{0.12}FeO_3$ addition resulting in an activity curve similar to that of $La_{0.88}Ag_{0.12}FeO_3$ alone (Fig. 6a). This blend of $La_{0.88}Ag_{0.12}FeO_3$ also promoted the ONCs formation as well as C_3H_6 conversion at oxygen close to stoichiometry (Fig. 6b and c). This can be ascribed to the improvement of oxidizing properties, which facilitates the nitrate formation and propene oxidation, owing to the presence of perovskite.

At 10% oxygen, the $deNO_x$ activity of $La_{0.88}Ag_{0.12}FeO_3$ can be maintained after a dilution by alumina giving NO conversions around 30% at $T > 400$ °C (Fig. 7a), which are obviously higher than those for $La_{0.88}Ag_{0.12}FeO_3$ alone. This feature is not a mere dilution effect but a synergistic

effect of the alumina surface. This result indicates that the dilution of $La_{0.88}Ag_{0.12}FeO_3$ by alumina is another effective way to use perovskite-based catalysts for lean NO_x reduction. The lower deNO_x activity at excess oxygen of M(1P-9A) compared to that of Ag/Al_2O_3 was corresponding to the low Ag content of the former. The scarcity of Ag-O-Al local structure, previously proposed to be crucial for lean NO_x reduction [11], is another likely reason for their low NO conversions with respect to Ag/Al_2O_3.

5 Conclusion

$La_{1-x}Ag_xFeO_3$ perovskites were prepared by reactive grinding having specific surface areas within the range of 30–40 m^2/g. γ-Al_2O_3 and Ag/Al_2O_3 prepared from boehmite possess surface areas of ~140 m^2/g. The redox properties of these materials were investigated by O_2-TPD and H_2-TPR reflecting an excellent oxidizing characteristic of perovskite-based catalysts, different from the poor oxidation ability of alumina-based samples. The oxidizing ability of the prepared catalysts follows the order of $La_{0.88}Ag_{0.12}FeO_3 > LaFeO_3 >> Ag/Al_2O_3 > Al_2O_3$. $LaFeO_3$ was found to be a suitable material for NO catalytic reduction at approximately stoichiometric oxygen (1% O_2), whereas, an excess of oxygen (10% O_2) led to a total inhibition of NO conversion over this catalyst. The same increase in O_2 content facilitated however the NO reduction over Al_2O_3. These catalytic performances accordingly correspond to the distinct redox properties of $LaFeO_3$ and Al_2O_3. The incorporation of Ag into $LaFeO_3$ lattice increased the number of anion vacancies (adsorption sites for NO and O_2), yielding an improvement in NO abatement by facilitating ONCs formation and C_3H_6 transformation by α-O_2. As for the alumina-based catalysts, supported Ag can accelerate the nitrate formation leading to a better deNO_x activity. The redox properties as well as the catalytic performance can be adjusted by using a blend of perovskite-type and alumina-based oxides. A synergistic effect was found after blending $La_{0.88}Ag_{0.12}FeO_3$ and Al_2O_3 which yields a bi-component catalyst showing deNO_x activity at both stoichiometric and excess oxygen as well as high C_3H_6 conversions at 1% O_2. A good performance of NO reduction at high oxygen concentration was also achieved via the addition of more reducing agent to compensate for that consumed by the combustion process.

Acknowledgments Financial support of NSERC through its industrial chair program is gratefully acknowledged. The authors thank Nanox Inc. for the preparation of the perovskite samples.

References

1. Bosch H, Janssen F (1988) Catal Today 2:369
2. Pischinger S (2004) Top Catal 30/31:5
3. Jansen WPA, Harmsen JMA, van der Gon AWD, Hoebink JHBJ, Schouten JC, Brongersma HH (2001) J Catal 204:420
4. Chin Y-H, Alvarez WE, Resasco DE (2000) Catal Today 62:291
5. Libby WF (1971) Science 171:499
6. Tejuca LG, Fierro JLG (1989) Adv Catal 36:237
7. Zhang RD, Villanueva A, Alamdari H, Kaliaguine S (2006) J Catal 237:368
8. Zhang RD, Villanueva A, Alamdari H, Kaliaguine S (2006) Appl Catal A Gen 307:85
9. Zhang RD, Villanueva A, Alamdari H, Kaliaguine S (2006) Appl Catal B: Environ 64:220
10. Zhang RD, Alamdari H, Kaliaguine S (2007) Appl Catal B: Environ 72:331
11. Miyadera T, Yoshida K (1993) Chem Lett 9:1483
12. Meunier FC, Zuzaniuk V, Breen JP, Olsson M, Ross JRH (2000) Catal Today 59:287
13. She X, Flytzani-Stephanopoulos M (2006) J Catal 237:79
14. Bethke KA, Kung HH (1997) J Catal 172:93
15. He H. Zhang RD, Yu YB, Liu JF (2003) Chin J Catal 24:788
16. Meunier FC, Ukropec R, Stapleton C, Ross JRH (2001) Appl Catal B: 30:163
17. Delahay G, Coq B, Ensuque E, Figueras F (1996) Catal Lett 39:105
18. Haneda M, Kintaichi Y, Inaba M, Hamada H (1998) Catal Today 42:127
19. Jen H-W (1998) Catal Today 42:37
20. Wichterlova B (2004) Top Catal 28:131
21. Kaliaguine S, van Neste A (2000) US patent 6017504
22. Otsuka K, Takahashi R, Yamanaka I (1999) J Catal 185:182
23. Cowan AD, Cant NW, Haynes BS, Nelson PF (1998) J Catal 176:329
24. Tanaka T, Okuhara T, Misono M (1994) Appl Catal B: Environ 4:L1
25. Royer S, van Neste A, Davidson R, McIntyre S, Kaliaguine S (2004) Ind Eng Chem Res 43:5670
26. Kaliaguine S, van Neste A, Szabo V, Gallot JE, Bassir M, Muzychuk R (2001) Appl Catal A: Gen 209:345
27. Porta P, De Rossi S, Faticanti M, Minelli G, Pettiti I, Lisi L, Turco M (1999) J Solid State Chem 146:291
28. Richter M, Bentrup U, Eckelt R, Schneider M, Pohl M-M, Fricke R (2004) Appl Catal B: Environ 51:261
29. Iglesias-Juez A, Hugría AB, Martínez-Arias A, Fuerte A, Fernández-García M, Anderson JA, Conesa JC, Soria J (2003) J Catal 217:310
30. Meunier FC, Breen JP, Zuzaniuk V, Olsson M, Ross JRH (1999) J Catal 187:493
31. Zhang RD, Alamdari H, Kaliaguine S (2006) J Catal 242:241
32. Zhang RD, Villanueva A, Alamdari H, Kaliaguine S (2006) J Mol Catal A: Chem 258:22